

Figure 1. (a) Description of the FFM measurement strategy. The DC tip position is a constant. This is due to real time application of a feedback force determined through a control loop after measurement of the tip position. Piezodither enforces an AC tip oscillation with 1 nm of free oscillation amplitude. A_{osc} and Φ are the measured quantities. (b), Static force measured between a brand new silicon AFM tip and a plane silicon sample during approach (blue) and retract (red) by FFM in presence of a capillary bridge. The linear behavior is fitted using the approximate solution given by J.Crassous et al. in Ref.[8] with $R=14\text{nm}$ and $r_k=12\text{nm}$.

the determination of the stiffness interaction and the associated dissipation following these linear equations (see details in Ref.[11]):

$$G' = F_r [n \cos(\Phi) - \cos(\Phi_\infty)] \quad (2)$$

$$G'' = \frac{F_r}{\omega} [-n \sin(\Phi) + \sin(\Phi_\infty)] \quad (3)$$

Φ is the phase shift between excitation at the lever clamped end and the tip oscillation. n is the normalized amplitude of tip vibration i.e. the measured amplitude at

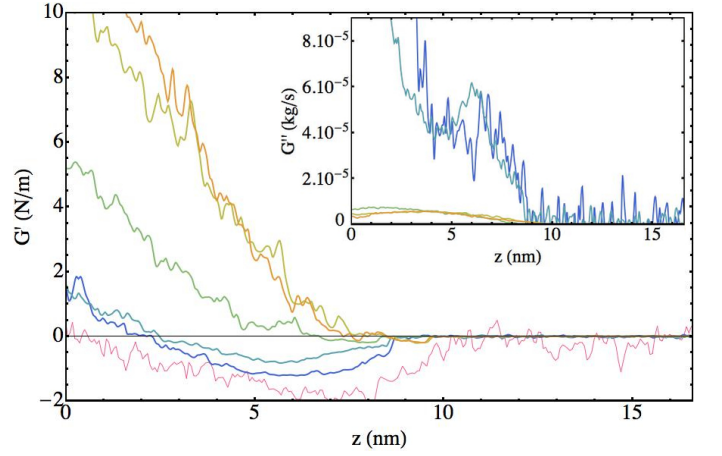


Figure 2. From blue to orange curves (respectively 300 Hz, 1 kHz, 44 kHz, 94 kHz and 114 kHz) show interaction stiffness, G' versus tip surface distance as deduced from experimental measurements using Eq.2. Red curve is the negative of the numerical derivative of the measured static force as the tip is pulled away from the surface. Inset: $G''(\text{kg/sec})$ result from Eq.3. It characterizes the mechanical energy dissipation increase during tip oscillation due to the capillary bridge. G'' at high frequencies is distinctively decreased as compared to G'' at low frequencies. Dissipation when in the thermodynamical equilibrium is clearly much higher.

distance z divided by the measured amplitude when tip is far away from the surface. At large distance $n=1$. In the experimental environment used (normal conditions in air), values of F_r and Φ_∞ are directly obtained from the system transfer function when the tip is far from the surface.

$$F_r = [(k - m\omega^2)^2 + c^2\omega^2]^{1/2} \quad (4)$$

$$\Phi_\infty = \arctan[(c/m)\omega/(\omega^2 - \omega_0^2)] \quad (5)$$

In the used frequency range with first resonance at 74,330kHz, a single mode description of the lever dynamics is sufficient. The stiffness of the lever k is obtained from measurement of the Brownian motion. The damping coefficient c and ω_0 (and therefore m) are obtained from lever transfer function measurement when the tip is far from the surface. F_r and Φ_∞ determined using this method are inserted in Eq.2 and 3 to obtain G' and G'' from n and Φ . In Fig.2, $k=2 \text{ N/m}$, $c=2.49 \cdot 10^{-8} \text{ kg/sec}$ and $\omega_0/2\pi=74,330\text{kHz}$.

Fig.2 shows that the visco-elastic coefficients exhibit a strong variation as the excitation frequency is varied over close to 3 orders of magnitude: G' varies from -1N/m up to 10N/m (therefore from negative to positive). The positive stiffness measured at high frequency, $G'=+10\text{N/m}$ is a very high interaction stiffness in AFM field. It is surprisingly observed associated to water and to an intense attractive static force close to 10nN . From this apparent

positive stiffness, although only surface effects due to the nano-meniscus are at work, an effective Young modulus E can be formally deduced: $E = G'z/\pi r_b$. It is in the range 0.1-1 GigaPa and increases as the tip moves closer to the surface.

At $\omega/2\pi=300\text{Hz}$, the measured interaction stiffness G' corresponds to the numerical derivative of the static force versus distance (i.e. the derivative of the red curve in Fig.1(b)). Here $\omega\tau \ll 1$ and the water nanobridge appears in thermodynamical equilibrium. However, the gradual increase of the excitation frequency leads to an important increase of the interaction stiffness, which finally becomes positive at all investigated distances [12]. The high frequency regime with positive and high stiffness is therefore an out of equilibrium behavior of the water droplet. As determined by use of Eq. 1, an estimate of the bridge relaxation time τ is 10^{-6}sec : the water molecule exchange between liquid and gas diminishes as the frequency increases toward 1MHz. This ultimately leads to a regime with a water nanobridge that has a constant volume. With this hypothesis of constant volume at high frequency, we analyze the observed positive stiffness G' due to the water nano-meniscus properties. This in fact follows analysis of Lambert et al in Ref.[13] produced for far larger water bridge (millimeter range). Equation 6 shows the expression of the total force due to the water nano-meniscus on the tip:

$$F = 2\pi r_b \gamma \sin(\theta) - 2H\pi r_b^2 \gamma \quad (6)$$

The force decomposes in two terms. The first term of Eq.6 is due to the tension associated to the contact line whereas the second is due to the Laplace pressure. γ is the water surface tension, $2\pi r_b$ the length of the circular contact line (or triple line), ($2H=1/\rho-1/r$) and θ , the angle between the water bridge and the surfaces. At thermodynamic equilibrium ($\omega\tau \ll 1$) with efficient evaporation condensation processes, whatever the tip surface distance and the oscillation amplitude, H is a negative constant. The pressure inside the bridge then does not change, and the contact line moves to accommodate this constrain of constant curvature as the tip surface distance is varied. During shortening of the bridge ($\delta h < 0$), the radius r_b increases as a result of the bridge spreading: the resulting stiffness $\delta F/\delta h$ is negative as observed experimentally. At $\omega\tau \gg 1$, we consider that the nanobridge volume remains constant. If the contact line does not move, the radius r_b is constant and the curvature increases ($H < 0$) as described in Fig.3(a). The second term in the force then provides a contribution to stiffness that is:

$$\frac{\delta F}{\delta h} = -2\pi r_b^2 \gamma \frac{\delta H}{\delta h} \quad (7)$$

This $\delta F/\delta h$ is then a positive contribution, which explains the origin of the positive stiffness experimentally observed.

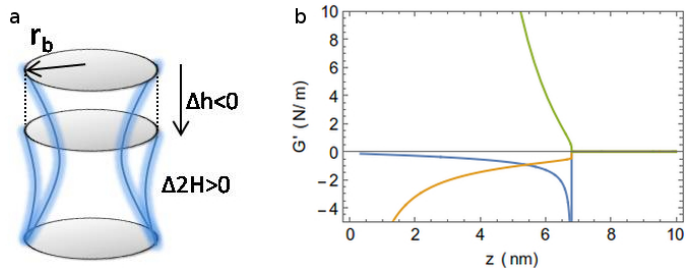


Figure 3. (a), evolution of the capillary bridge shape as the gap decreases at constant volume and at locked contact line. (b), results from numerical calculation, reproduce the key experimental features obtained using Force Feedback Microscopy at different frequencies. At low frequency (blue curve), the signature of the thermodynamical equilibrium is again obtained with a negative stiffness at all distances. At high frequency oscillation (green curve), the water nanobridge is at constant volume and the contact line is immobile. A positive stiffness is obtained like in experimental results. It is however significantly above all measured stiffnesses for which, at $\omega\tau=0.7$, contact line mobility is reduced but certainly far from zero. The orange curve represents a regime at constant volume, but with a contact line free to move. It leads to a negative stiffness. This regime, which implies a curvature only marginally varying, cannot explain the experimental observations at high frequency.

A numerical calculation of the stiffness G' in the three extreme regimes (thermodynamical equilibrium, constant volume with locked contact line or free to move contact line) is reported in Fig.3(b).

Finally as shown in inset of Fig.2, $G''(\text{kg}/\text{sec})$, the dissipative part of the linear response, is found to decrease as the excitation frequency increases and as G' severely increases. This leads us to conclude that this change of G'' is also determined by the contact line behavior. A mobile contact line on the AFM tip then appears to be associated to an important dissipation. As mobility of the contact line decreases, this channel of energy dissipation closes and G'' diminishes accordingly. Although only surface effects are here at work, G'' can be formally analyzed as an apparent volume viscosity: $G'' \propto \eta R$, where $R=14\text{nm}$ is the tip size. In that case, with a typical $G''=10^{-5} \text{ kg}/\text{sec}$ here measured and taken equal to ηR , η is in the range $10^2-10^3 \text{ Pa}\cdot\text{sec}$. This is orders of magnitude above $\eta=10^{-3} \text{ Pa}\cdot\text{sec}$, the bulk value of water viscosity(Ref.[14, 15]).

In conclusion, for the first time, two different viscoelastic regimes in dynamical properties of a water nanobridge are measured. The major result is that, despite the fact that the static interaction between surfaces associated to capillary bridges is always attractive, an apparent and highly positive stiffness appears at the nanoscale when the two surfaces interact with a short characteristic time, whereas, the friction measured in same conditions, is found strongly reduced. A description can be proposed to simultaneously explain these

results. Contrary to the situation at thermodynamical equilibrium with condensation and evaporation, in the out of equilibrium regime, any displacement of the line can only be ensured by a flow in the nanodroplet. The sticky boundary condition leads to a diverging shear velocity as the water film thickness goes to zero close to the triple line. In this situation, moving the line becomes extremely difficult. Indeed, we observe in the diminution of G'' , at high frequencies a drop of the line mobility. In this case, at constant volume, there is then no alternative: the curvature of the nano-meniscus must change, which we observe in the increase of G' .

The frequency ranges in our experiments are the ones used to operate AFM in dynamical mode. Results presented here will certainly have to be considered in the daily analysis of dynamic mode AFM experiences when

a water nanobridge is present. Due the importance of the observed changes in effective visco-elastic properties of water at nanoscale, this conclusion is certainly not limited to AFM but opens a broader perspective, as capillary bridges are now known to be important in surface interactions not only at different scales but also at different time scales.

ACKNOWLEDGMENTS

Mario S. Rodrigues and Miguel V. Vitorino acknowledge financial support from Fundação para a Ciência e Tecnologia, grants SFRH/BPD/69201/2010 and PD/BD/105975/2014 respectively.

-
- [1] William Thomson. 4. on the equilibrium of vapour at a curved surface of liquid. *Proceedings of the Royal Society of Edinburgh*, 7:63–68, 1872.
- [2] Elisa Riedo, Francis Lévy, and Harald Brune. Kinetics of capillary condensation in nanoscopic sliding friction. *Physical review letters*, 88(18):185505, 2002.
- [3] Jérôme Crassous. *Etude d'un pont liquide de courbure nanométrique: propriétés statiques et dynamiques*. PhD thesis, 1995.
- [4] Edward Lansing Cussler. *Diffusion: mass transfer in fluid systems*. Cambridge university press, 2009.
- [5] D Rugar, HJ Mamin, and Peter Guethner. Improved fiber-optic interferometer for atomic force microscopy. *Applied Physics Letters*, 55(25):2588–2590, 1989.
- [6] Mario S Rodrigues, Luca Costa, Joël Chevrier, and Fabio Comin. Why do atomic force microscopy force curves still exhibit jump to contact? *Applied Physics Letters*, 101(20):203105, 2012.
- [7] Luca Costa, Mario S Rodrigues, Simon Carpentier, Pieter Jan van Zwol, Joël Chevrier, and Fabio Comin. Comparison between atomic force microscopy and force feedback microscopy static force curves. *arXiv preprint arXiv:1306.2775*, 2013.
- [8] Jérôme Crassous, Matteo Ciccotti, and Elisabeth Charlaix. Capillary force between wetted nanometric contacts and its application to atomic force microscopy. *Langmuir : the ACS journal of surfaces and colloids*, 27(7):3468–73, April 2011.
- [9] Mika M Kohonen and Hugo K Christenson. Capillary condensation of water between rinsed mica surfaces. *Langmuir*, 16(18):7285–7288, 2000.
- [10] This measured value of r_k is higher than expected based on vapor pressure. We have not controlled the hygrometry level during numerous experiments. We estimate an average value of hygrometry of 50 per cent. This would lead to a Kelvin radius r_k clearly smaller than 5nm. A hygrometry level close to 99 per cent is required to observe a Kelvin radius of about 12nm. This is certainly not our case. It is however known that with no special treatment of the used silicon surfaces, large Kelvin radii are commonly observed, see previous reference. $r_k=12\text{nm}$ is the value we have used to determine the characteristic time.
- [11] Mario S Rodrigues, Luca Costa, Joël Chevrier, and Fabio Comin. System analysis of force feedback microscopy. *Journal of Applied Physics*, 115(5):054309, 2014.
- [12] At $w=44\text{kHz}$ and above, the measured stiffness reaches values between 6N/m and 10N/m. Direct contact between the tip and a hard surface with Pauli repulsion at work, could be responsible for such a high stiffness. All curves presented in Fig. 2 have been measured during pulling the tip away from the surface. At all frequencies, we used exactly the same experimental conditions: tip control, lever oscillation amplitude, and overall time to acquire data along a complete approach/retract force curve. We simultaneously measured the static force and the dynamic response, so that we know at each point, what is the DC tip position in the static force curve shown in Fig. 1(b). The same conditions, at identical tip surface distance, with comparable oscillation amplitude, lead to a negative stiffness at low frequencies and to a positive one at high frequency. We then conclude that this increase is a direct consequence of the water bridge dynamical properties and that at high frequencies, the water bridge becomes much stiffer.
- [13] J-B Valsamis, Massimo Mastrangeli, and Pierre Lambert. Vertical excitation of axisymmetric liquid bridges. *European Journal of Mechanics-B/Fluids*, 38:47–57, 2013.
- [14] Using small-amplitude AFM based technique, variations of dynamical properties of a confined liquid such as a comparable increase of the stiffness, have been reported in Ref.15. This leads authors to conclude that bulk properties of water are changed by confinement close to a surface. These reports are related to change in molecular structure of liquid layers whereas in our case, the nano-meniscus behavior is the key. In Ref.15, the tip is immersed into the bulk liquid. There is no nano-meniscus due to a gas-liquid interface. The strong reported variations occur when the tip-surface distance is below 1nm, as in our case the relevant separations are between 1nm and 10nm.
- [15] Shah H Khan, George Matei, Shivprasad Patil, and Peter M Hoffmann. Dynamic solidification in nanoconfined water films. *Physical review letters*, 105(10):106101, 2010.